

# Characterization of defects at grain boundaries of GaP and InP by infrared cathodoluminescence

F. Domínguez-Adame and J. Piqueras

Departamento de Física de Materiales, Facultad de Ciencias Físicas, Universidad Complutense, 28040 Madrid, Spain

(Received 11 July 1990; accepted for publication 10 September 1990)

Grain boundaries in GaP and InP have been studied by infrared cathodoluminescence (CL). In GaP the results indicate that there exists a depletion region beside grain boundaries where the concentration of  $P_{Ga}$  antisite defects is lower than in the bulk material. In InP the near-edge CL emission and a deep level luminescence at 1.07 eV have been found to cause similar grain boundary CL contrast.

The properties of grain boundaries in semiconducting materials are of interest due to their influence on carrier mobility or lifetime and to the use of polycrystalline semiconductors in devices as solar cells and microwave generators. Several techniques based on the scanning electron microscope as the emissive mode, cathodoluminescence (CL), electron beam induced current (EBIC), and scanning electron acoustic microscopy (SEAM) have been used in the past to characterize grain boundaries in III-V materials. CL and EBIC contrast of grain boundaries mainly arises from local inhomogeneities of the space distribution of point defects or impurities near the boundaries. While grain boundaries show a high contrast in the visible-CL images, a weak SEAM contrast has been observed in GaP and InP boundaries.<sup>1</sup> In the present work infrared-CL is used to study grain boundaries in polycrystalline GaP and InP. CL of boundaries, in the visible range, has been previously described<sup>1,2</sup> in the case of GaP.

The materials used in this investigation are polycrystalline GaP and InP from Metals Research and nominally undoped. From the original rods of about 30 mm diameter, samples of approximately  $5 \times 5 \times 2 \text{ mm}^3$  were cut perpendicular to the axis of the rod. The samples were then mechanically and chemically polished and subsequently observed in the emissive and CL modes in a Hitachi S-2500

or a Cambridge S4-10 SEM, at an accelerating voltage of 30 keV and beam currents of  $10^{-7}$ – $10^{-6}$  A. An optical lens was used to concentrate the light on a photomultiplier tube or a cooled North Coast Ge detector for the ranges of 350–800 nm and 0.8–1.8  $\mu\text{m}$ , respectively, attached to a window of the microscope. In some cases CL images for wavelengths above 1  $\mu\text{m}$  were recorded by adapting a cut-on optical filter at the detector entrance. To record spectra a light guide feeding the light to an Oriel 78215 computer-controlled monochromator was used. The relative efficiency of the system as a function of wavelength was calibrated against a calibrated standard lamp. All the measurements were performed at 160 K.

Figure 1 shows the spectrum of GaP in the visible range. The experimental conditions for observation of the near-edge green luminescence and of the red band at about 700 nm (1.77 eV) in the SEM have been previously described.<sup>3,4</sup> The spectrum in the near-infrared region shows a broad band at about 1200 nm (1.03 eV) as seen in Fig.

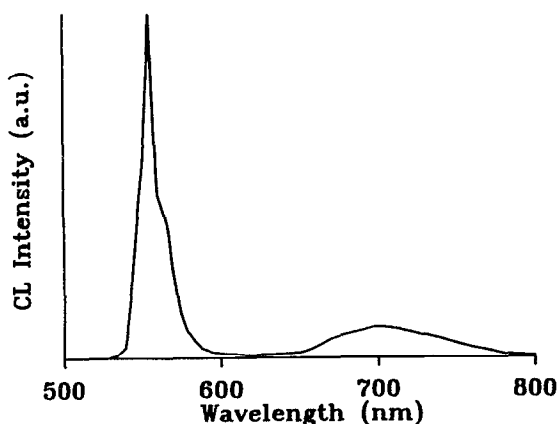


FIG. 1. Visible CL spectrum of a GaP sample recorded at 160 K.

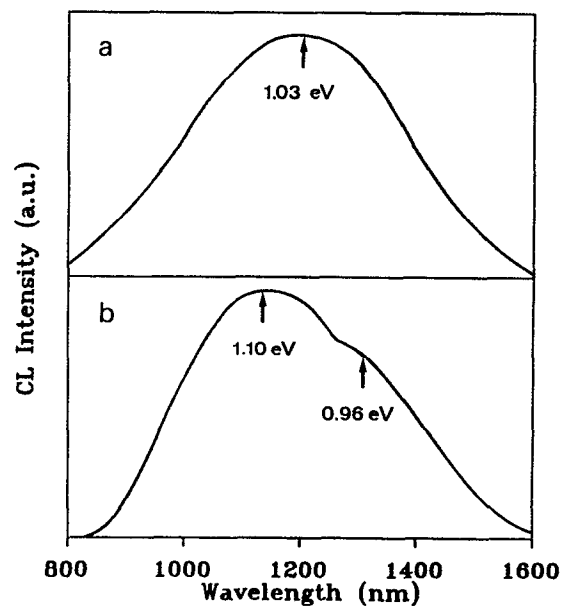


FIG. 2. Near-infrared CL spectrum of the same sample as in Fig. 1 obtained with (a) focused electron beam and (b) defocused beam.

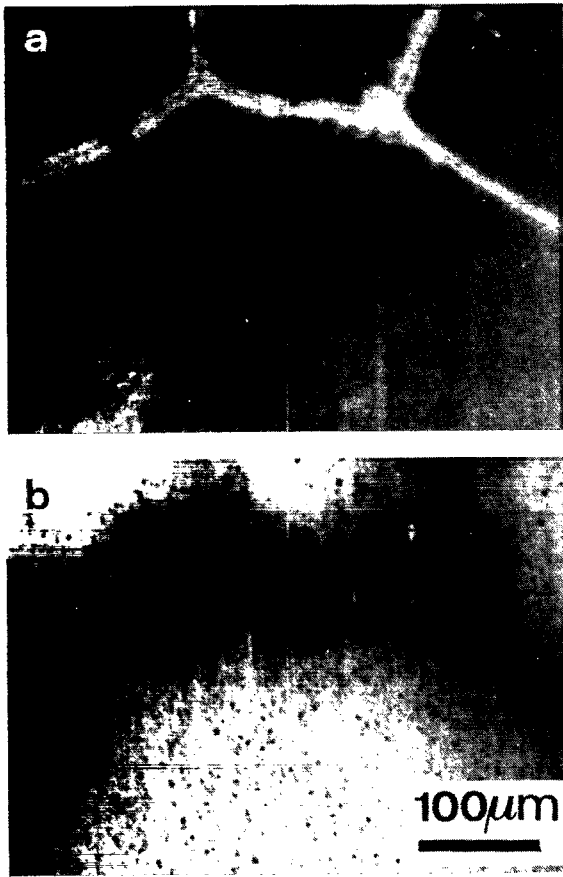


FIG. 3. (a) Visible and (b) near-infrared (wavelength above 1000 nm) CL images of the same area of a GaP sample.

2(a); by defocusing the electron beam the spectrum of Fig. 2(b) is recorded. The position of the emission bands does not change when the spectra are recorded inside and outside grain boundaries. Figure 3 shows the visible and infrared CL images of the same boundary in GaP. The visible-CL image shows the central dark line surrounded by green-emitting bright bands previously described.<sup>2</sup> The

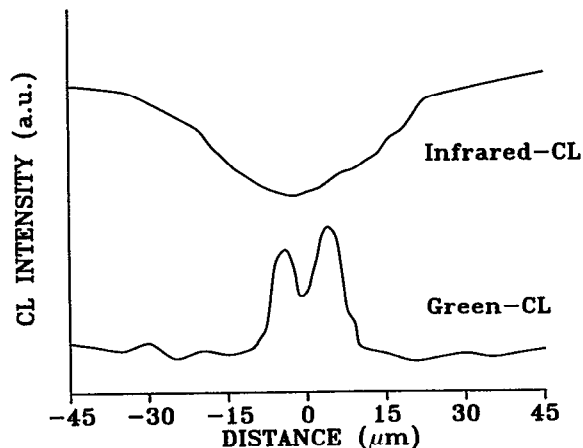


FIG. 4. Line scan of CL intensities for the visible and infrared emissions across a grain boundary in GaP.

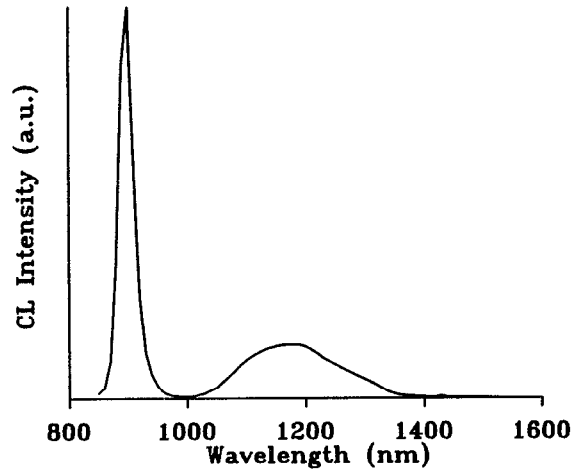


FIG. 5. Near-infrared CL spectrum of an InP sample.

near-infrared image, however, shows a dark band of nearly constant width [Fig. 3(b)], indicating that the 1.03 eV emission is lower close to the boundaries than in the bulk material. Line scans of CL intensities across the grain boundary are depicted in Fig. 4.

Spectra from InP samples (Fig. 5) show a near-edge-band peak centered in 891 nm (1.393 eV) with full width at half maximum (FWHM) of 40 meV, and a broad band (FWHM of 180 meV) centered at about 1160 nm (1.07 eV), indicating the occurrence of deep levels. The relative emission of the deep center band is enhanced by lowering the excitation conditions, just as occurs for the red band in GaP.<sup>3</sup> No difference was observed in the spectra recorded inside and outside the boundaries. Figure 6(a) shows the monochromatic ( $\lambda = 891$  nm) CL image from an InP sample. Dark grain boundaries are observed but appear crossed by a dense array of dark lines, related to polishing damage (indicative of the difficulties inherent in polishing InP crystals<sup>5</sup>). Nearly the same contrast is observed in images recorded by using the 1  $\mu\text{m}$  cut-on filter [Fig. 6(b)].

Infrared-CL studies of GaP have not been numerous but deep levels have been studied in the past by photoluminescence techniques. An infrared band, close to the 1200 nm observed in this work, has been found by Killoran *et al.*<sup>6</sup> in as-grown GaP crystals. They report on a composite infrared band with emissions at 1130 nm (1.10 eV) and 1275 nm (0.97 eV) associated to different recombination processes involving the  $\text{P}_{\text{Ga}}$  antisite defect. This composite character would explain the dependence of the infrared band on the excitation conditions we have observed in this work. Infrared-CL images of GaP single crystals show that the contrast at dislocations is about inverse to that of the visible CL,<sup>7</sup> suggesting that  $\text{P}_{\text{Ga}}$  antisites concentrate near the dislocation core. A similar, although not complete, inversion is found at grain boundaries, so we suggest that there exists a depletion region of about 20  $\mu\text{m}$  beside the boundary where the concentration of  $\text{P}_{\text{Ga}}$  antisite defects is lower than in the bulk material. No new radiative recombination centers appear near grain boundaries, as concluded from the absence of spectral variations inside and outside the boundaries.

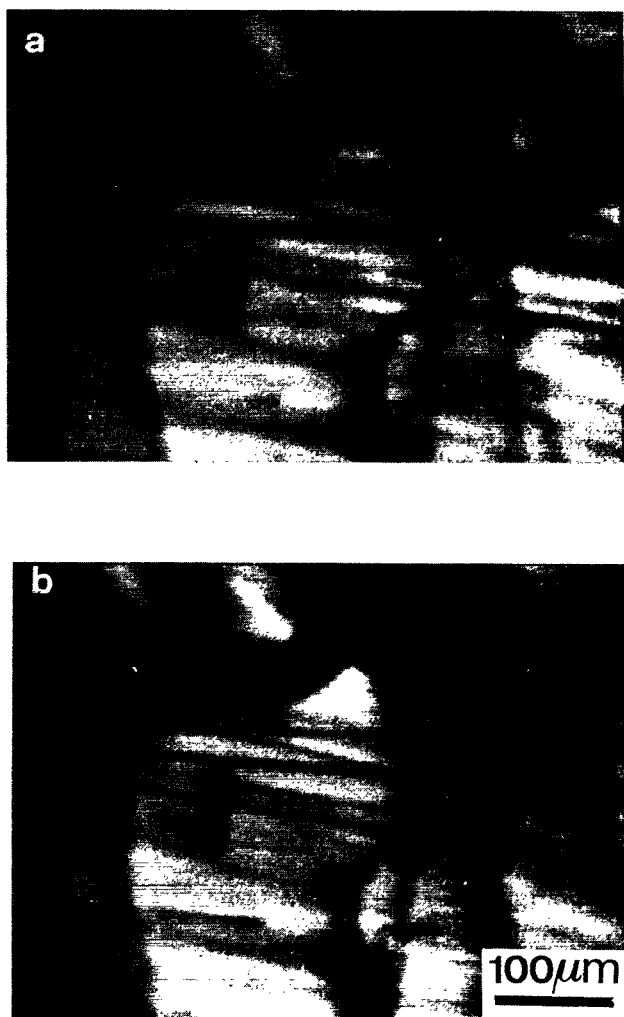


FIG. 6. (a) Near-edge-band (wavelength of 891 nm) and (b) deep-level-band (wavelength above 1000 nm) CL images of the same area in InP.

Grain boundaries in InP appear as dark lines in the infrared-CL images for both near-edge and deep-level-band emissions. Although such a correspondence between near-edge and deep-level luminescence images on InP has not been, to our knowledge, previously described, it seems that

grain boundaries cause the same effect on CL as dislocations. This is apparent in the fact that dislocations show a dark spot contrast<sup>8-10</sup> in the near-edge and total luminescence images, and in the observation<sup>11</sup> that the CL spectra inside the dislocations and in the bulk are similar. Concerning the origin of the deep-level band, Temkin *et al.*<sup>12,13</sup> reported the existence of a vacancy-impurity broad band (FWHM of 160 meV at 100 K) centered at about 1150 nm (1.078 eV) in melt-grown InP. The authors suggested that the vacancy involved is on the P sublattice. A similar band with a maximum at 1158 nm (1.07 eV) and a FWHM ranging from 110 meV at 35 K to 215 meV at room temperature, was found by Myhajlenko *et al.*<sup>11</sup> in CL spectrum of heat-treated LEC InP. We suggest that our band of 1160 nm (1.07 eV) is that previously reported in Refs. 11, 12, and 13.

Finally, in order to compare the capabilities of CL and SEAM techniques it can be mentioned that twinned regions in the samples of GaP and InP used here are readily observed by means of SEAM.<sup>1</sup> However, we have not been able to image such regions with the infrared-CL technique in this work. It appears that the influence of twin boundaries on the segregation of point defects is negligible compared to that of the grain boundaries.

This work was partially supported by the Comisión Interministerial de Ciencia y Tecnología (Project PB86-0151) and by DGICYT-DAAD.

<sup>1</sup>F. Domínguez-Adame and J. Piqueras, *J. Appl. Phys.* **66**, 2751 (1989).

<sup>2</sup>J. Llopis and J. Piqueras, *Phys. Status Solidi A* **49**, K9 (1978).

<sup>3</sup>F. Domínguez-Adame, J. Piqueras, N. de Diego, and J. Llopis, *J. Appl. Phys.* **63**, 2583 (1988).

<sup>4</sup>F. Domínguez-Adame and J. Piqueras, *Mater. Chem Phys.* **21**, 539 (1989).

<sup>5</sup>M. Cocito, P. Franzosi, G. Salviati, and F. Taiariol, *Scanning Electron Microsc.* **IV**, 1299 (1986).

<sup>6</sup>N. Killoran, B. C. Cavenett, M. Godlewski, T. A. Kennedy, and N. D. Wilsey, *J. Phys. C* **15**, L723 (1982).

<sup>7</sup>F. Domínguez-Adame, J. Piqueras, and P. Fernández (unpublished).

<sup>8</sup>K. Böhm and B. Fischer, *J. Appl. Phys.* **50**, 5453 (1979).

<sup>9</sup>M. Cocito, C. Papuzza, and F. Taiariol, *Inst. Phys. Conf. Ser. No. 67*, 273 (1983).

<sup>10</sup>A. K. Chin, S. Mahajan, and A. A. Ballman, *Appl. Phys. Lett.* **35**, 784 (1979).

<sup>11</sup>S. Myhajlenko, J. L. Batstone, H. J. Hutchinson, and J. W. Steeds, *J. Phys. C* **17**, 6477 (1984).

<sup>12</sup>H. Temkin and W. A. Bonner, *J. Appl. Phys.* **52**, 397 (1981).

<sup>13</sup>H. Temkin, B. V. Dutt, W. A. Bonner, and V. G. Keramidis, *J. Appl. Phys.* **53**, 7526 (1982).